



AEROCAPTURE NAVIGATION AT NEPTUNE

Robert J. Haw
Jet Propulsion Laboratory

AAS/AIAA Astrodynamics Specialists Conference

Big Sky Resort, Big Sky, Montana, August 3-7, 2003

AAS Publications Office, P.O. Box 28130, San Diego, CA 92198

AEROCAPTURE NAVIGATION AT NEPTUNE

Robert J. Haw*

A proposed Neptune Orbiter Aerocapture mission will use solar electric propulsion to send an orbiter to Neptune. Navigation feasibility of direct-entry aerocapture for orbit insertion at Neptune is shown. The navigation strategy baselines optical imaging and Δ VLBI measurements in order to satisfy the flight system's atmosphere entry flight path angle, which is targeted to enter Neptune with an entry flight path angle of -11.6° . Error bars on the entry flight path angle of ± 0.55 (3σ) are proposed. This requirement can be satisfied with a data cutoff 3.2 days prior to arrival. There is some margin in the arrival template to tighten (*i.e.* reduce) the entry corridor either by scheduling a data cutoff closer to Neptune or alternatively, reducing uncertainties by increasing the fidelity of the optical navigation camera.

INTRODUCTION

An orbiter mission is described combining solar electric propulsion for an inter-planetary transfer to Neptune and aerocapture technology for orbit insertion upon reaching Neptune. This paper evaluates the feasibility of navigating a direct-entry aerocapture at Neptune. The work is part of a NASA inter-center study [Ref 1].

Aerocapture is an orbit insertion flight maneuver within a planetary atmosphere using drag to decelerate the spacecraft to orbital velocities with a single pass through the atmosphere. It requires zero or minimal propellant to effect the orbit insertion. Aerocapturing into a closed elliptical orbit around Neptune has the advantage of allowing higher entry velocities than would otherwise be possible, thus reducing the interplanetary transfer time. It also reduces arrival mass for a given payload mass.

An established accuracy requirement for the navigation sub-system did not exist at the time of this study. One of the purposes of this work then, was to set limits on the navigation error and, in collaboration with aerocapture colleagues [Ref 1], determine aerocapture accuracy requirements for navigation.

An error analysis requires detailed inputs in order to build the navigation model, so first a representative spacecraft proposed by the aerocapture study group is described [Ref 2 & 3], followed by a description of the target selection and mission design. Several system trades are subsequently performed, including a trade on entry velocity at Neptune.

REPRESENTATIVE SPACECRAFT CONFIGURATION

The orbiter is enclosed by an aeroshell. The mass of the entire entry flight system is 1800 kg (including propellant load). The lift-to-drag ratio (L/D) of the vehicle equals 0.6 and its ballistic coefficient ($M/C_D A$) is approximately 150 kg/m^2 .

* Jet Propulsion Laboratory, California Institute of Technology, Pasadena, CA 91009. Email: robert.haw@jpl.nasa.gov. Telephone: 818-354-2567.

The spacecraft is modeled as a 3-axis-fixed spacecraft with momentum-wheel ACS stabilization. The momentum wheels maintain spacecraft pointing, and balanced thrusters perform periodic momentum de-saturation burns.

Solar electric propulsion (SEP) boosts the package after launch. SEP thrusts within the inner solar system, but all engines and solar arrays are discarded beyond ~3 a.u. The propulsion system remaining after jettisoning the SEP is a mono-propellant hydrazine system. This subsystem performs the momentum wheel de-saturations and trajectory correction maneuvers (TCMs) during the approach to Neptune.

The telecommunications sub-system during the interplanetary transfer employs a Ka (or possibly X) -band high gain antenna (HGA) mounted on the back of the aeroshell for telemetry and navigation. The HGA is a 1 m diameter dish antenna, with a 5 watt transmitter and a gain of 36dBi. At 30 a.u. the data rate to a 70 m ground antenna is ~100 bps. Also mounted on the aeroshell are forward-looking cameras for optical navigation.

The tracking and telemetry sub-system will use a Small Deep Space Transponder, which supports phase coherent two-way doppler and ranging, command signal demodulation and detection, telemetry coding and modulation, and differential one-way range (DOR) tone generation (for Δ VLBI measurements).

TARGET SELECTION

The Neptune target is determined by the post-insertion orbit, atmosphere characteristics, and the aerodynamic performance of the entry vehicle.

The entry interface (EI) target at the top of the atmosphere consists of three parameters: inertial flight path angle (FPA), clock angle, and radius. The flight path angle is the angle subtended by the vehicle trajectory with the local horizontal at the entry interface radius (see Appendix 1). The FPA used for this study is -11.6° [Ref 1]. The clock angle, as its name suggests, is a clockwise angular measure of the position of the target point on the projected face of Neptune's disk, measured from the T axis (see Appendix 2). The entry interface radius is defined to be 25,757.0 km (an altitude 1000 km above the 1 bar ambient pressure level) [Ref 1].

The entry interface target and desired orbit characteristics are provided in Table 1.

Table 1
ENTRY INTERFACE TARGET AND
POST-INSERTION ORBIT CHARACTERISTICS
Entry time: 2021 April 28 00:09 UTC

EI Target (Retrograde Entry)				Initial Orbit Characteristics		
Altitude (km)	Latitude (deg)	eFPA (deg)	Entry Velocity (km/s)	Altitude (km)	Inclination (deg)	Period (hours)
1000	7N	-11.6	28.0	4000* x 430,000	157	80

* After the pericenter-raise maneuver

TRAJECTORY OVERVIEW

A pair of Neptune trajectories was chosen to perform trades. The pair is representative of a single interplanetary trajectory found by Sauer and Noca [Ref 4]. The two trajectories are equivalent except for their hyperbolic excess velocity. The v_{∞} 's are 15.9 km/s and 18.5 km/s.

The vehicle arrives at Neptune on April 28, 2021 after a journey of 10 or more years. The range to Earth at entry is 29.8 a.u. (one-way light time equals 4 hours).

The approach trajectory is ballistic. The entry is retrograde, making the atmosphere-relative velocity at the EI significantly higher than for a prograde entry. A retrograde entry imposes rigorous requirements on the flight system (high decelerations and heat loadings) but the subsequent capture orbit is preferable because it facilitates rendezvous with Triton (inclination equal to 157° and orbit period of 5.9 days). Alternatively, as shown in Reference 5, a prograde entry is less demanding on the flight system but penalizes the mission with long period orbits (on the order of months) and expensive inclination changes (to align the spacecraft with Triton's orbit). The retrograde option was chosen for this study.

Reference 5 recommends an entry velocity near 29 km/s. Trades are performed here on entry velocities of 28 km/s and 30 km/s, corresponding to $v_\infty = 15.9$ km/s and 18.5 km/s respectively.

The entry vehicle enters the atmosphere at an altitude of 1000 km above the 1 bar level and descends to ~ 200 km before climbing and exiting the atmosphere. Near apocenter, a pericenter-raise maneuver is performed to raise pericenter out of the atmosphere. See Figure 1. The Δv needed to raise pericenter to an altitude of 4000 km is 90 m/s. A 4000 km pericenter lies well above the atmosphere but still satisfies Neptune-science measurement objectives [Ref 6].

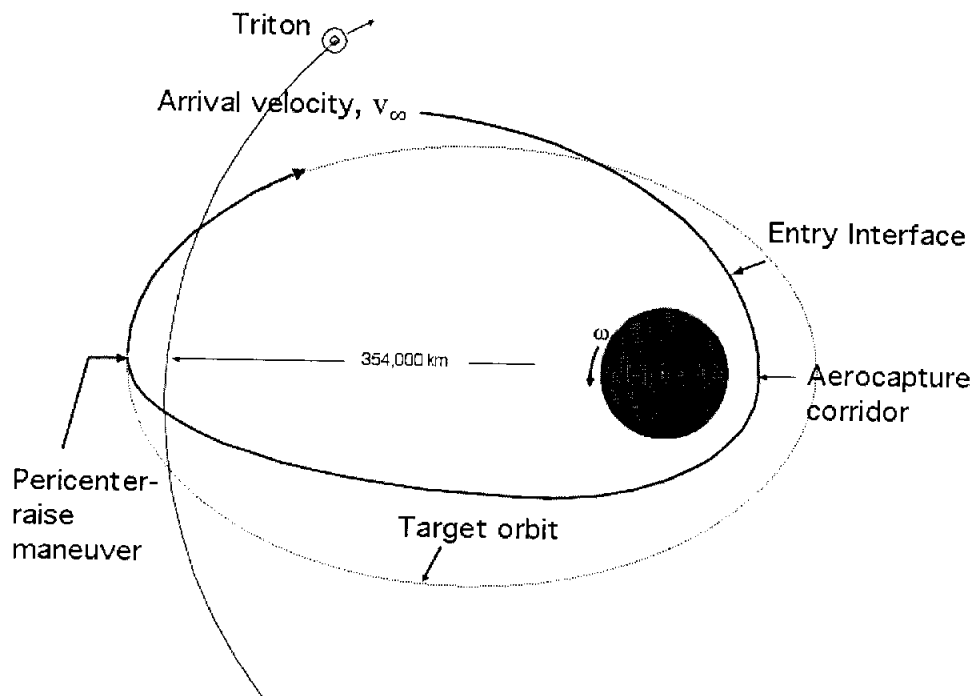


Figure 1 Schematic of Neptune Aerocapture

An entry velocity of 28 km/s decelerates the orbiter with a unit force of $\sim 5 \pm 3$ g's and slows the vehicle ~ 6 km/s by the time of egress. At 30 km/s the mean deceleration is ~ 8 g's [Ref 3].

Short period orbits around Neptune (days, rather than months) are desirable for science objectives. In addition to yielding more science quantitatively, short period orbits have relatively low hyperbolic velocities -- an advantage for tour design and for observing Triton (assuming apocenter is greater than

Triton's orbit). Tour design benefits because gravity assist swing-bys are more efficient at low velocities (inverse-square relationship between trajectory-bending and v_{∞}). Triton observations benefit because longer exposure times are possible. Therefore Triton approach velocities should be kept as low as practical.

The orbit radius of Triton is 354,000 km. Using the previous considerations as guidance, an apocenter equal to 430,000 km was selected to satisfy science requirements and orbit commensurability. This distance defines an orbit period of 80 hours and a 7:4 resonance with Triton [Ref 7].

AEROCAPTURE

Entry flight path angle is constrained by the physical limitations of the flight system (the vehicle must withstand aerodynamic, structural, and heat loads), and by the need to accumulate sufficient drag forces to slow the spacecraft (to avoid skipping-out). Error bars on the entry trajectory define a corridor through the atmosphere.

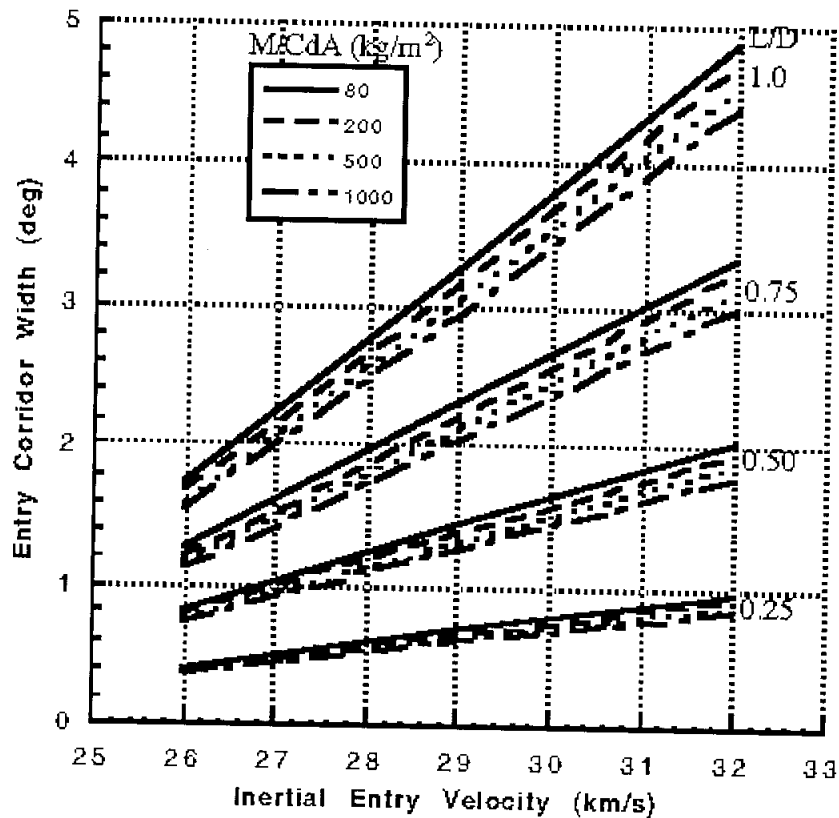
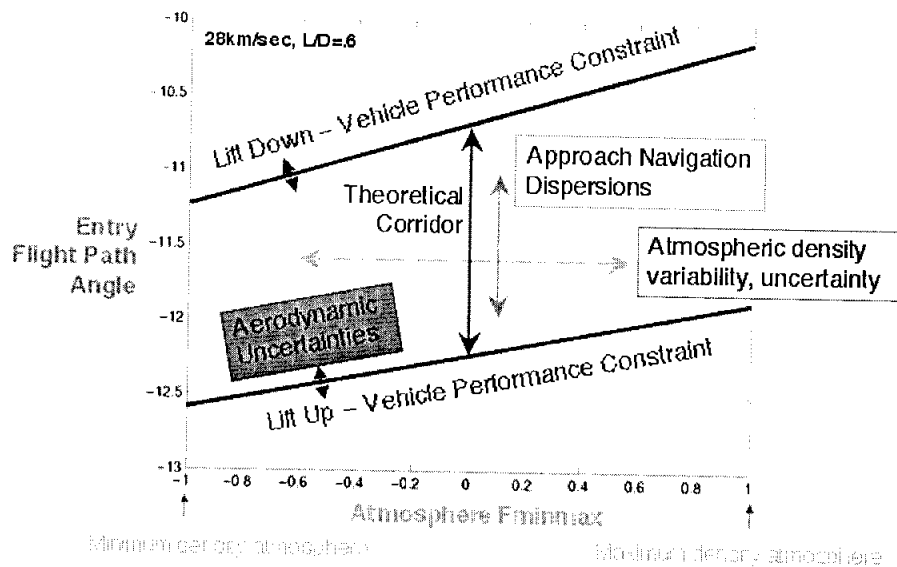


Figure 2 Variation of Entry Corridor Width as a Function of Entry Velocity and Ballistic Coefficient. Apocenter = 400,000 km [Ref 5]

The diameter of the corridor through the atmosphere represents the maximum total uncertainty that can be accumulated by the vehicle -- with contributions from the atmosphere, vehicle aerodynamics, and navigation. Corridor diameter defines the maximum tolerable limits along the aerocapture flight path.

Reaching the desired apocenter then, is a function of adjusting entry velocity, L/D , and ballistic coefficient. In Figure 2 entry corridor width is plotted versus entry velocity for a range of ballistic coefficients bounding representative vehicle sizes. (Note that this figure applies to an apocenter radius of 400,000 km and not 430,000 km.) For the vehicle used here and an entry velocity of 28 km/s, Figure 2 indicates a theoretical corridor width of $\sim 1.4^\circ$ (*i.e.* $\pm 0.70^\circ$) while an entry velocity of 30 km/s specifies a theoretical width of $\sim 2.0^\circ$ (*i.e.* $\pm 1.0^\circ$). Higher entry velocities provide additional margin but subject the vehicle to greater stress.

The errors contributing to a corridor width corresponding to an entry velocity of 28 km/s and a vehicle L/D of 0.6 are shown in Figure 3. The abscissa represents atmosphere variability, where the dimensionless parameter F_{minmax} varies from minimum atmospheric density (-1) through maximum density (1).



**Figure 3 Vehicle Performance for Apocenter = 430,000 km
E-3 day Delivery [Ref 3]**

Navigation dispersions contribute approximately 77% of the corridor uncertainty in Figure 3 for F_{minmax} equal to -1 (the narrowest point). Conservatively assuming the same proportional contribution in the center of the plot at F_{minmax} equal to 0, a flight path angle requirement appropriate to levy on navigation will be 77% of 1.4° or a 3σ error of approximately $\pm 0.55^\circ$ for an entry velocity of 28 km/s, and a 3σ error of approximately $\pm 0.75^\circ$ for an entry velocity of 30 km/s. (Note that the corridor width in Figure 3 defines 100% values although it has been asserted here that the limits represent 3σ values. This equivalence is inconsistent but is not troubling because the margins for error in this analysis are greater.)

NAVIGATION DATA

The navigation accuracy achievable at the destination, or target, is established at the final control point along a trajectory (*i.e.* the last maneuver before reaching say, Neptune) and is usually termed the delivery accuracy, or simply the *delivery*. Since there is a limit on the accuracy with which an initial state and subsequent dynamics are known, the future state cannot be computed with complete certainty from an

initial one. So a delivery at time T includes the future uncertainty expected in the spacecraft state (at its time of arrival[♦]) computed at time T, where T is before the time of arrival. That is, an E-2 day delivery represents the prediction of the location of the spacecraft at Neptune, when still 2 days away from Neptune.

The error analysis undertaken here begins at Neptune-90 days.

Ephemeris Determination

Ephemeris errors dominate the navigation errors at Neptune and an aerocapture mission isn't feasible unless these errors are reduced significantly. Neptune's ephemeris errors, as well as Earth's, are given in Table 2. This tabulation is given in a Sun-centered RTN coordinate system, where R represents radial direction from the Sun, T down-track direction (the direction of motion of Neptune in its orbit), and N the out-of-plane direction.

Table 2
NEPTUNE AND EARTH EPHEMERIS UNCERTAINTIES (3 σ)
Mapped to 2021

Central Body	R (km)	DT (km)	OOP (km)	TOTAL (RSS)
Earth	0.01	3	4	5
Neptune*	10,200	12,000	5,200	16,000
Neptune**	3,400	4,000	1,733	5,200

* DE405 (circa 2000)

** Uncertainties used for this analysis

The second line in Table 2 represents the error in Neptune's position in 2021 as currently projected by JPL's DE405 planetary ephemeris (*i.e.* a mapping of 21 years). (In an absolute sense these errors are large, but the total error is only about one-third the planet's diameter.) Significant improvements to the ephemeris between now and 2021 can be expected. As more observations are acquired between now and arrival, *a priori* errors will decrease. For example, the Neptune *a priori* ephemeris error for Voyager II was ~5000 km RSS (3 σ). For this analysis the assumed *a priori* error are one-third the DE405 errors. Those errors are shown on the third line in Table 2.

Optical Data

Target-relative imaging is important in this mission because of the uncertainty in the location of Neptune. Optical navigation data are used to reduce Neptune's errors. These data consist of digital images of Neptune and its satellites, set in front of a stellar background. The background stars, combined with Neptune's ephemeris, establish the spacecraft-Neptune relative position by astrometry.

The optical navigation campaign begins at E-75 days. Ground-based facilities will process the transmitted pictures to extract the optical observables, and the data will be combined with radiometric measurements. Data processing and observable-extraction require approximately eight hours to complete (as of 2003).

Transmissions will be constrained by the down-link data rate (~100 bps). A schedule of one image per every four hours (6 pictures per day) satisfies this constraint.

Early in the approach phase, one picture every other day is shuttered, alternating between Neptune and Triton. The picture frequency increases to six per day within 16 days of Neptune. This yields approximately 170 images in the complete optical data set.

♦ More specifically, 'entry time', defined in Table 1.

The imaging system envisioned here follows a design similar to the Mars Reconnaissance Orbiter optical navigation camera. Relevant technical specifications of the MRO camera are: aperture = 6 cm, focal length = 50 cm, field-of-view = 1.4° per side, detector = 1024x1024 CCD array, pixel resolution = 50 μrad, mass = 2.7 kg, peak power = 4 W [Ref 8]. Higher performance cameras will yield better results. Therefore an advanced camera (“MRO plus”) with a pixel resolution of 40 μrad is also parameterized to show relative performance.

For comparison with an operating mission, the Cassini wide-angle navigation camera has these specifications: aperture = 6 cm, focal length = 20 cm, field-of-view = 3.5° per side, detector = 1024x1024 CCD array, pixel resolution = 60 μrad, mass = 27 kg, peak power = 35 W [Ref 9]. The MRO camera offers higher resolution than Cassini, yet weighs less and operates with less energy (but has a smaller field-of-view).

See Appendix 3 for other camera parameters.

Tracking Data

Navigation tracking data consists of two-way and three-way coherent Ka-band doppler and range measurements. (X-band data were found to perform equally as well.) These data are augmented during approach with optical observations and interferometry.

Interferometry enhances the solution relative to that achievable with doppler, range and optical data (although optical data dominates in a ranking of the relative importance of the four data types). In general though, interferometric data *i.e.* Delta Differenced One-way Range (Δ DOR), has limited effectiveness at the range of Neptune, although it can be used to some advantage in combination with the other data types. That is, while optical data determines plane-of-sky information for Neptune (from which the plane-of-sky position of the spacecraft can be inferred), Δ DOR measurements can determine plane-of-sky spacecraft components directly.

Δ DOR measurements are not constrained by the down-link, but require 24 hours to extract the observable from the data (conservatively).

Data schedules used in this analysis for doppler, range and Δ DOR are provided in Table 3. Data measurement accuracies are listed in Appendix 3.

Table 3
DOPPLER & RANGE TRACKING AND Δ DOR MEASUREMENTS

Start	End	Radiometric Coverage	Start	End	Δ DOR Observations
E-90days	E-60	2 tracks/week			
E-59	E-45	1 track /day	E-75days	E-51	1 per week
E-44	E-17	2 tracks/day	E-50	E-31	3.5 per week
E-16	Entry	3 tracks/day	E-30	Entry	14 per week

NAVIGATION MODEL

Significant error sources in the navigation model are noted in the sub-sections below. Appendix 3 lists all error sources and *a priori* uncertainties.

Maneuver Placement

Maneuvers during the approach phase were placed as shown in Table 4 below. This is a representative schedule put together for the purposes of the error analysis. The last targeting maneuver during approach is the most sensitive to placement, for it defines the delivery accuracy. For this reason two opportunities are shown in Table 4 for the final targeting maneuver: E-2 days and E-1 day. For the baseline strategy (E-2 days) the data cutoff is 3 days from Neptune, whereas the alternative strategy proposes a data cutoff 2 days from Neptune. The alternative strategy delivers smaller uncertainties but leaves less time to correct those errors before entry.

Table 4
NEPTUNE ORBITER TCMs

TCM*	Time**	Data Cutoff**	Description
TCM1	E -60 days	E - 65 days	Correct SEP cruise errors.
TCM2	E -10 days	E - 15 days	Penultimate targeting
TCM3	E - 2 days	E - 3 days	Ultimate targeting
TCM3'	E - 1 day	E - 2 days	Ultimate targeting (alternate)
TCM4	~E +0.75 day	~E + 0.1 day	Apocenter correction
TCM5	~E +1.75 day	~E + 0.85 day	Pericenter-raise to 4000 km

*Numbered starting at the beginning of the approach phase.
**With respect to entry (E) time.

All maneuvers in Table 4 except TCM5 are statistical maneuvers. The statistical analysis necessary to size the statistical maneuvers has not been performed, but the mean Δv for TCM1 and TCM2 probably will not exceed 1 m/s (based on the ephemeris errors). The expected Δv for either TCM3 or TCM3' will be greater (but it is not expected to be more than an order of magnitude greater). The deterministic component of the TCM5 magnitude is 90 m/s.

Orbit Determination

The dominant orbit determination uncertainties consist of ephemeris errors, TCM execution uncertainties, and data errors. The uncertainties contributing to orbit determination errors are listed in Appendix 3.

RESULTS

Delivery errors are a combination of orbit determination errors and maneuver execution errors, mapped to the entry interface. Sensitivity trades in this sub-section look at optical navigation and/or ΔDOR observations, delivery time, ephemeris errors, and entry velocity.

Delivery uncertainties are plotted in Figure 4 below. Neptune's ephemeris uncertainty is the predominant reason for the large uncertainties at the left edge of the figure.

Figure 4 illustrates six options, or strategies. Option 1 is the baseline case: *i.e.* MRO-like camera with 6 pictures per day maximum, plus doppler, range and ΔDOR .

Option 2 doubles the number of pictures acquired by the camera during the last two weeks of approach (an unlikely scenario given the assumed down-link rate). This option shows appreciable improvement with respect to Option 1. Option 3 suggests the benefits that an advanced camera (MRO-plus) may offer. Its performance (with 6 pictures per day) is equivalent to Option 2 (with 12 pictures per

day). Option 4 lacks Δ DOR measurements. Some degradation occurs with this loss but the degradation is not significant. The loss of Δ DOR can be balanced by substituting the advanced camera. Option 5 illustrates the performance of the Cassini wide-angle camera. It does not perform as well as the baseline case. Option 6 illustrates the inappropriateness of performing this mission with only doppler and range data.

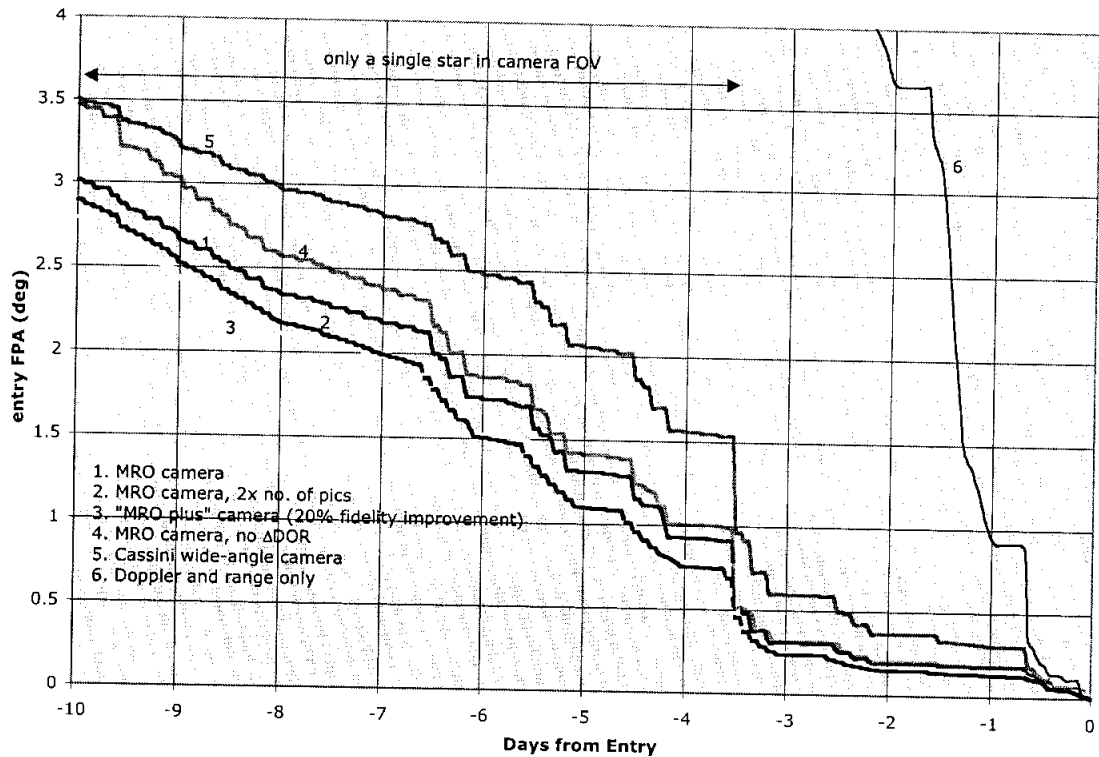


Figure 4 FPA v. Time-to-Go (3σ)
Entry Velocity = 28 km/s

The geometry of this trajectory lacks bright background stars suitable for optical navigation (*i.e.* few are visible behind Neptune). The navigation information content per image is enhanced with multiple background stars, but a narrow field of view reduces the probability of capturing more than a single bright star. (Multiple stars determine the center point of Neptune more accurately because of the additional degrees-of-constraint introduced.) The camera performances shown in Figure 4 are not optimum because only a single star is visible per image until E-3.5 days. At that time a second star enters the field-of-view, and the improvement in the delivery is significant.

Sensitivities are shown in Tables 5 - 8. The entries in Tables 5 and 6 reproduce Figure 4 in greater detail at selected times. Note that FPA entries in these tables don't mirror values from Figure 4 at those selected times. The processing time for computing optical and Δ DOR observables introduces a lag during flight operations. That lag has been accounted for in Tables 5 and 6, but is not computed in Figure 4. That is, Figure 4 represents instantaneous processing of optical and Δ DOR measurements. For Tables 5 - 8, processing delays of 10 hours for optical data and 24 hours for Δ DOR are assumed.

Tables 5 and 6 show that the proposed delivery requirement is satisfied at the time of Delivery B (E-3 days) for all of the tracking options with cameras. (Except for the Cassini option which narrowly misses.)

Table 5
DELIVERY ACCURACY (3 σ)
28 KM/S

	Doppler & Range Only	Doppler Range & Optical	Doppler Range Optical Δ DOR	Doppler Range Optical Δ DOR
Proposed Req'm't	± 0.55	± 0.55	± 0.55	± 0.55
Delivery A				2x pics
Data Cutoff at E-4.25 days		145 pics	145 pics	213 pics
Semi-major axis (km)	1152	234	222	183
Semi-minor axis (km)	591	84	57	51
Ellipse angle (deg)	67	21	24	22
Entry time (s)	117	36	33	27
B magnitude (km)	720	222	217	171
Flight Path Angle (deg)	± 4.5	± 1.5	± 1.3	± 1.1
Delivery B				2x pics
Data Cutoff at E-3 days		153 pics	153 pics	229 pics
Semi-major axis (km)	1122	84	81	60
Semi-minor axis (km)	588	63	48	42
Ellipse angle (deg)	68	35	23	20
Entry time (s)	114	12	12	9
B magnitude (km)	702	78	78	60
Flight Path Angle (deg)	± 4.4	± 0.48	± 0.48	± 0.37
Delivery C				2x pics
Data Cutoff at E-2 days		159 pics	159 pics	241 pics
Semi-major axis (km)	1011	57	45	36
Semi-minor axis (km)	534	39	36	27
Ellipse angle (deg)	76	65	49	59
Entry time (s)	102	6	6	6
B magnitude (km)	582	42	39	30
Flight Path Angle (deg)	± 3.7	± 0.27	± 0.24	± 0.18
Parameter Update				2x pics
Data Cutoff at E-12 hours		168 pics	168 pics	258 pics
Semi-major axis (km)	885	36	33	27
Semi-minor axis (km)	30	18	18	15
Ellipse angle (deg)	93	102	98	98
Entry time (s)	3	3	3	2
B magnitude (km)	33	18	18	15
Flight Path Angle (deg)	± 0.21	± 0.11	± 0.11	± 0.09

Table 6
CAMERA SENSITIVITY (3 σ)
28 KM/S

	MRO camera (baseline)	MRO camera (baseline) 2x pics	MRO plus camera	Cassini camera
Proposed Req'm't	± 0.55	± 0.55	± 0.55	± 0.55
Delivery B				
Data Cutoff at E-3 days	153 pics	229 pics	153 pics	153 pics
Semi-major axis (km)	81	60	66	153
Semi-minor axis (km)	48	42	42	75
Ellipse angle (deg)	23	20	23	23
Entry time (s)	12	9	9	24
B magnitude (km)	78	60	63	144
Flight Path Angle (deg)	± 0.48	± 0.37	± 0.39	± 0.89

Table 7 shows the effect of improvements to the *a priori* Neptune ephemeris. There are no significant improvements. That is, the delivery is not sensitive to ground-observation updates to the ephemeris *i.e.* the current planetary ephemeris DE405 is satisfactory. This is an unexpected result, but verifies the value of the optical navigation.

Table 7
ENTRY FPA -- EPHEMERIS SENSITIVITY (3 σ)
28 KM/S

Neptune ephemeris ->	Baseline circa 2021	DE405 (mapped to 2021)
Data Cutoff		
E - 3 days (deg)	± 0.48	± 0.49
E - 2 days (deg)	± 0.24	± 0.25
E - 12 hours (deg)	± 0.11	± 0.11

Table 8 shows that entry flight path angle uncertainty is proportional to entry velocity, as expected.

Table 8
ENTRY FPA -- ENTRY VELOCITY SENSITIVITY (3 σ)

Data Cutoff	28 km/s	30 km/s
E - 3 days (deg)	± 0.48	± 0.79
E - 2 days (deg)	± 0.24	± 0.36
E - 12 hours (deg)	± 0.11	± 0.20

Flight path angle dispersions shown in Table 8 are plotted versus entry velocity in Figure 5.

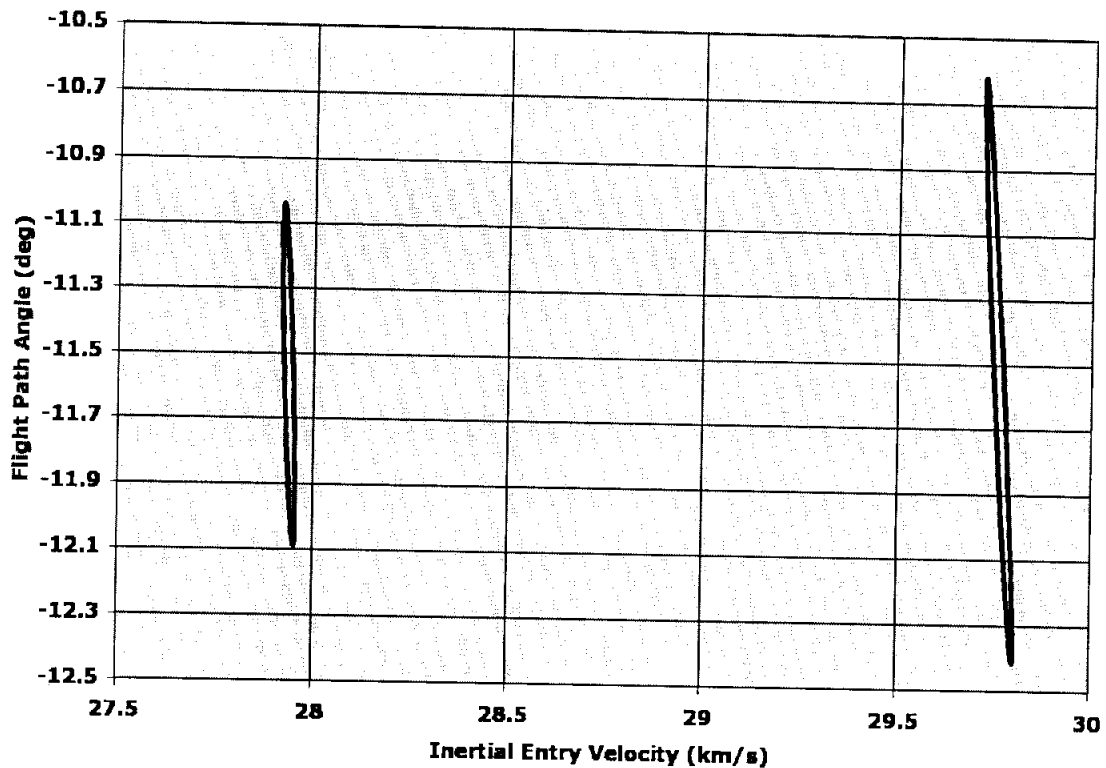


Figure 5 Navigation Dispersions for 28 km/s and 30 km/s at EI (99%)
E-3 day Delivery

DISCUSSION

Optical Navigation Data

This mission cannot be performed without optical navigation. Moreover even with optical navigation little margin appears to exist in the navigation sub-system. For the nominal case under consideration (MRO-like camera, picture frequency = 6 per day), the delivery requirement is satisfied at about E-3.2 days. An additional day can be purchased, *i.e.* delivery at about E-4 days, by employing a camera more advanced than the MRO version (MRO-plus) or by increasing the downlink rate to support a higher picture frequency. This strategy offers modest improvements, although the sensitivity to further camera development is evident.

A more likely source to find immediate additional paper margin is from a well-designed picture sequence command file. The picture sequence file used in this analysis captured multiple stars only for the last 3.5 days, and the effect (the difference between a single and multiple stars) is significant and self-evident (see Figure 4 again). Thus with detailed optical navigation planning, the delivery requirement could be satisfied by ~E-4.5 days for the nominal case or as early as ~E-5 days for the advanced camera (by extrapolation in Figure 4).

Navigation images of Neptune, because of its atmosphere, have relatively large uncertainty (especially during the two weeks preceding entry). This uncertainty was mitigated by incorporating pictures of Triton because airless bodies do not degrade optical data in a way that an atmosphere does. (A ratio of 2 Triton pictures for every 1 Neptune picture was used here.)

The *a priori* ephemeris of Neptune is not important to the delivery. The mission can be undertaken with the current DE405 ephemeris and the current Triton *a priori* ephemeris.

Tracking Data

Δ DORs and optical data are orthogonally complementary and combine to yield plots 1, 2, 3 and 5 in Figure 4. Plot 3 assumes an advanced camera (MRO-plus) and represents the best delivery in the current study (but <7% improvement over the baseline). Note that plot 2 is similar to plot 3, but represents a less advanced camera shuttering at twice the frequency.

Δ DOR measurements improve delivery accuracy <5% after accounting for the data processing lag (instantaneously the improvement is ~10%). Improvement is possible because Δ DOR observations are sensitive to state errors along components insensitive to doppler and range.

There is no advantage to using Ka-band doppler tracking in place of X-band. Small benefits were seen with Ka-band Δ DOR observations (*vis-a-vis* X-band observations), but the overall improvement to the delivery was insignificant.

Propellant Budget

As a rough estimate of propellant loading, at least 105 m/s of velocity change is required to get into orbit (*i.e.* not including on-orbit maintenance propellant nor the allocation necessary to perform a Neptune-Triton orbital tour). The 105 m/s total is composed of ~12 m/s of pre-insertion statistical Δv and a deterministic $\Delta v = 90$ m/s for TCM5 (the pericenter-raise maneuver – note: the statistical component of this maneuver is still TBD). An additional statistical maneuver (TCM4) is needed between egress and apocenter (before TCM5) to correct residual aerocapture errors and achieve the apocenter target. The size of this maneuver is TBD. The 105 m/s total is expected to grow significantly with these TBD additions.

TCM4 and TCM5 are scheduled with only one day separating them, and both maneuvers must be designed and burned within ~40 hours of egress. This is a difficult, but not impossible task to accomplish using traditional maneuver template procedures (*i.e.* no autonomy).

Comparison with Other Missions

Entry FPA results (or expected results) from other missions are summarized in the table below. (MER, Stardust, and Huygens have not yet arrived at Mars, Earth, and Titan respectively at the time of this writing.)

Table 9
FPA DELIVERY COMPARISON (3σ)

Mission	Entry FPA	Delivery Error	Delivery Time	Reqm't
Neptune Orbiter	-11.6°	$\pm 0.24^\circ$	E-2 d	< ± 0.55 >
Titan Explorer*	-36.8°	$\pm 0.6^\circ$	E-2 d	< ± 1.0 >
Mars Pathfinder	-14.2°	$\pm 0.4^\circ$	E-2 d	± 1.0
MPL	-12.0°	$\pm 1.0^\circ$	E-2 d	$\sim \pm 0.5$
MER	-11.5°	$\pm 0.2^\circ$	E-2 d	± 0.25
Stardust	-8.2°	$\sim \pm 0.8^\circ$	E-2 d	± 0.80
Galileo probe	-8.6°	$\pm 0.6^\circ$	E-140 d	± 1.4
Huygens probe	-64.0°	$\pm 3.0^\circ$	E-21 d	± 3.4

* Proposed mission. See Reference 10.

<-> denotes proposed requirement.

MPL and Stardust stand out in the short list above with high uncertainties.

The MPL mission was characterized by unbalanced and mis-modeled thrusting activities. The level of thrusting required by the ACS system to maintain attitude significantly exceeded pre-launch expectations, and this mis-modeling contributed to the entry flight path angle uncertainty shown in Table 9.

Huygens (the Cassini probe) anticipates a delivery uncertainty of $\pm 3.0^\circ$. This apparently large uncertainty nevertheless satisfies requirements. One reason for the large delivery error is the Titan ephemeris uncertainty. Another reason is the tour re-design Cassini has undergone recently [Ref 11].

The MER delivery, on the other hand, is significantly smaller than the Neptune Orbiter delivery. Mars' well-known ephemeris and MER's lower hyperbolic excess velocity are contributors to this improvement.

SUMMARY

This preliminary study has baselined the use of optical observations and Δ DOR measurements for delivering an aerocapture orbiter to Neptune. The study has also proposed a conservative entry FPA requirement of $\pm 0.55^\circ$ (3σ) based on delivery results that accommodate the aerocapture. The proposed delivery requirement is satisfied at E-3.2 days. This date can be pushed earlier in all likelihood (further from Neptune) with subsequent follow-up optimization of (i) the picture sequence file and (ii) camera design.

This study makes two recommendations to enhance performance at Neptune:

- Development of a targetable, advanced optical navigation camera. The MRO navigation camera currently under development represents a satisfactory technological readiness level, but an advanced version will buy margin.
- Second, incorporation of on-board autonomous maneuver capability.

Δ DOR measurements offer negligible benefit. This analysis does not support a navigation strategy incorporating Δ DOR measurements.

Proposed entry requirements can be met using the equivalent of a future DE405 *a priori* Neptune ephemeris such as that described in Table 2.

This work represents a first-cut effort at determining concept feasibility. Many simplifying assumptions were made, especially with respect to the optical data, in order to accomplish this study in a timely manner.

ACKNOWLEDGEMENT

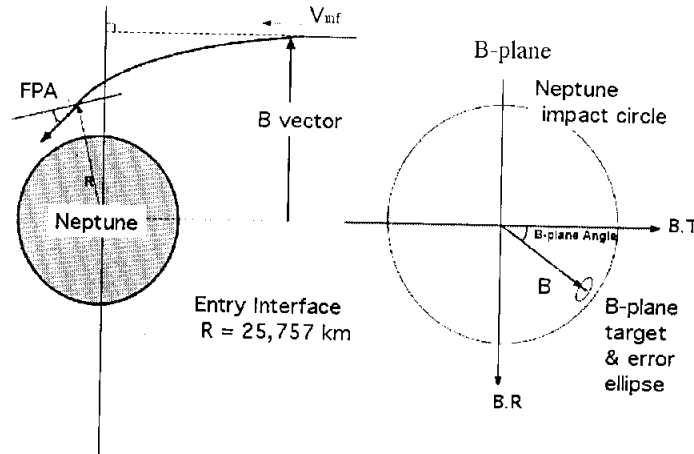
The work described in this paper was performed at the Jet Propulsion Laboratory, California Institute of Technology under contract from the National Aeronautics and Space Administration. The work was funded through the In-space Propulsion program.

The author would like to thank D.W. Way, M.K. Lockwood, B. Starr, J.L. Hall, W.M. Owen, and L.A. Cangahuala for helpful comments and support in preparing this paper. Carl Sauer constructed the initial SEP trajectory between Earth and Neptune.

REFERENCES

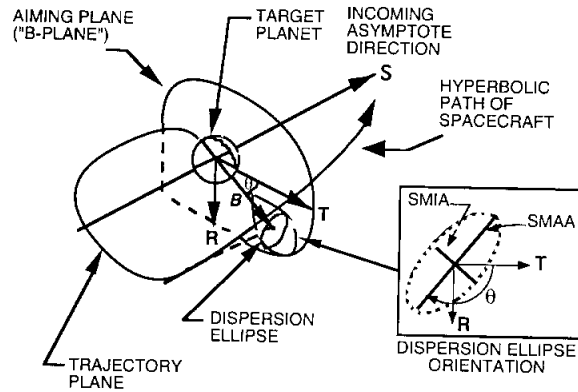
1. M.K. Lockwood, Langley Research Center. Team lead, "Neptune aerocapture systems analysis study group", NASA In-space Propulsion program, Oct. 2002 – Aug. 2003.
2. R.W. Bailey, JPL, private communication, Dec 2002.
3. M.K. Lockwood, D.W. Way, B. Starr, Langley Research Center, private communication and viewgraph presentations, Dec 2002 – April 2003.
4. C. Sauer, M. Noca, JPL, private communication, Sept 2002.
5. P.F. Wercinski, Y-K Chen, M. Loomis et al, "Neptune Aerocapture Entry Vehicle Preliminary Design" paper AIAA-2002-4812, AIAA Atmospheric Flight Mechanics Conference, Monterey, CA., Aug. 5-8, 2002.
6. R. Shotwell, T. R. Spilker, JPL, "Missions to Neptune and Triton in the Next Decade (2013-2023)", viewgraph presentation, Jan 24 2002.
7. R.W. Bailey, T.R. Spilker, R.J. Haw, JPL. Private communication and collaborative analysis, Dec. 2002 – Jan 2003.
8. G. Frascetti, JPL, "MRO Optical Navigation Camera Preliminary Design Review", viewgraph presentation, May 8 2002.
9. W.M. Owen, JPL, private communications, April 2002 - May 2003.
10. R.J. Haw, "Approach Navigation for a Titan Aerocapture Orbiter", paper AIAA-2003-4802, AIAA Joint Propulsion Conference, Huntsville Alabama, July 20-23, 2003.
11. N. Strange, T. Goodson, Y. Hahn, "Cassini Tour Redesign for the Huygens Mission", paper AIAA-2002-4720, AIAA Specialist Conference, Monterey Calif, 5-8 August 2002.

APPENDIX 1: FLIGHT PATH ANGLE AND B-PLANE



APPENDIX 2: B-PLANE DESCRIPTION

Planet or satellite approach trajectories are typically described in aiming plane coordinates referred to as “*B*-plane” coordinates (see Figure). The *B*-plane is a plane passing through the body center and perpendicular to the asymptote of the incoming trajectory (assuming two body conic motion). The “*B*-vector” is a vector in that plane, from the body center to the piercing-point of the trajectory asymptote. The *B*-vector specifies where the point of closest approach would be if the target body had no mass and did not deflect the flight path. Coordinate axes are defined by three orthogonal unit vectors, *S*, *T*, and *R*, with the system origin at the center of the target body. *S* is parallel to the spacecraft v_{∞} vector (approximately the velocity vector at the time of entry into the target body’s gravitational sphere of influence). *T* is arbitrary, but typically specified to lie in the ecliptic plane (the mean plane of the Earth’s orbit), or in the body equatorial plane. Finally, *R* completes an orthogonal triad with *S* and *T*.



Aiming Plane Coordinate System Definition

Orbit determination errors can be characterized by a statistical dispersion ellipse in the aiming plane (*B*-plane) and a statistical uncertainty along the *S* (down-track) direction. In the Figure, SMIA and SMAA denote the semi-minor and semi-major axes of the dispersion ellipse (*i.e.* 50% of the distance across the ellipse along the respective coordinate). The angle θ is measured clockwise from *T* to SMAA.

APPENDIX 3: A PRIORI NAVIGATION MODEL UNCERTAINTY

Error Source	A Priori Uncertainty (1σ)	Correlation Time	Comments
Data			
doppler (mm/s)	0.05 / 0.075	-	Ka-band (two-way / three-way doppler)
range (m)	5	-	Ka-band
Δ DOR (nrad)	2	-	0.055 ns (Ka-band)
optical (pixels) Triton only	0.25 - 0.5	-	minimum stellar magnitude limit = 7.5
Estimated Parameters			
epoch state			
position (km)	1000	-	
velocity (km/s)	1	-	
Neptune ephemeris (km) $\times 10^3$	(3.4, 4., 1.7)	-	R,AT,OOP (~ error at time of Voyager II)
doppler bias (mm/s)	0.0005	0	
range bias (m)	2	0	
clock bias (s)	1.0×10^{-8}	0	
camera pointing error (deg)	(0.25, 0.25, 2)	0	R.A., Dec, Twist; estimated per observation
non-gravitational accelerations (km/s^2)	2.0×10^{-12}	10 days	spherical covariance, estimated daily (1 day batches)
solar pressure	10%	-	reflectivity coefficient
ACS ΔV (mm/s), 1 per three weeks	(2, 2, 2)	-	(line-of-sight, lateral, normal) components
TCMs (mm/s)			spherical covariance
TCM-1	5	-	2% (3s) proportional error (per axis) 6 mm/s (3s) fixed error (per axis) 10 milli-radian proportional pointing error (per axis)
TCM-2	2	-	
TCM-3	15	-	
Earth pole direction (cm)	2 \rightarrow 5	0	(X and Y). Ramps to higher value during final week of data. (For UT1, ~5 cm \rightarrow 0.13 ms.)
UT1 (cm)	2 \rightarrow 5	0	
ionosphere - day (cm)	55	0	S-band values
ionosphere - night (cm)	15	0	
troposphere (cm)	1	0	
Considered Parameters			
station locations (cm)	3	-	
quasar locations (nrad)	2	-	for Δ DOR data